Available online at www.sciencedirect.com
SCIENCE DIRECT®
Pergamon
International Journal of Machine Tools & Manufacture 43 (2003) 1015–1022
INTERNATIONAL JOURNAL OF MACHINE TOOLS & MANUFACTURE
DESIGN, RESEARCH AND APPLICATION

An experimental investigation into the orthogonal cutting of unidirectional fibre reinforced plastics

X.M. Wang, L.C. Zhang *

School of Aerospace, Mechanical and Mechatronic Engineering, The University of Sydney, Sydney, NSW 2006, Australia

Received 22 March 2002; received in revised form 11 March 2003; accepted 14 March 2003

Abstract

This paper aims to understand the machinability of epoxy composites reinforced by unidirectional carbon fibres when subjected to orthogonal cutting. It was found that the subsurface damage and its mechanisms of a machined component are greatly influenced by fibre orientation. The material's bouncing back is a characteristic phenomenon associated with the cutting of a fibre-reinforced composite. Three distinct deformation zones appear, i.e., chipping, pressing and bouncing when the fibre orientation is $<90°$. Otherwise, fibre-bending during cutting will become more significant and subsurface damage caused by fibre-matrix debonding will be severer. As a result, surface roughness, subsurface damage and cutting forces all change dramatically with the fibre orientation. It was also found that the curing conditions of making the composites do not have an obvious effect on the machinability, though the mechanical properties of the materials vary.

Keywords: Orthogonal cutting; Unidirectional fibre; Composites; Machining damage; Surface integrity

1. Introduction

Fibre-reinforced plastics (FRPs) have been widely used in a variety of structures, such as aircraft, robots and machines. The applications require high quality machined surfaces, including dimensional accuracy and surface integrity. Because FRPs contain at least two phases of materials that possess very different mechanical properties, the mechanism of material removal is different from that of machining single-phased materials, such as metals. In the former, machining often causes severe damage represented by delamination, fibre pull-out, fibre-fragmentation, burning and fuzzing. However, compared to the machining of metals, the investigations on that of FRPs are insufficient and limited to some special applications, such as edge trimming [1,2], effects of tool materials and geometries [3,4], machining-induced structural integrity [5], size effect in orthogonal cutting [6] and mechanism of chip formation [7] and drilling [8]. Because of the complexity of the structure of FRPs, the deformation mechanisms of the materials under cutting are still far from deep understanding, even though a simply-structured composite was attempted [9]. No reliable cutting theory is available to guide the machining of FRPs.

This study aims to investigate the machinability of epoxy composites reinforced by unidirectional carbon fibres subjected to orthogonal cutting. It is expected that the simple structure of the composites particularly selected in this study will facilitate the understanding of the relations among machining conditions, surface integrity and the microstructure and manufacturing conditions of the composites.

2. Experimental

A surface grinder, MININI M286, was modified for the cutting experiment, with the grinding wheel being replaced by a cutting tool. The hydraulic table of the machine, on which an FRP specimen was held, provided a steady cutting motion. The cutting forces were measured by a three-dimensional dynamometer, Kistler

* Corresponding author. Tel.: +61-2-9351-2835; fax: +61-2-9351-7060.
E-mail address: zhang@mech.eng.usyd.edu.au (L.C. Zhang).

0890-6955/03/$ - see front matter © 2003 Elsevier Science Ltd. All rights reserved.
doi:10.1016/S0890-6955(03)00090-7

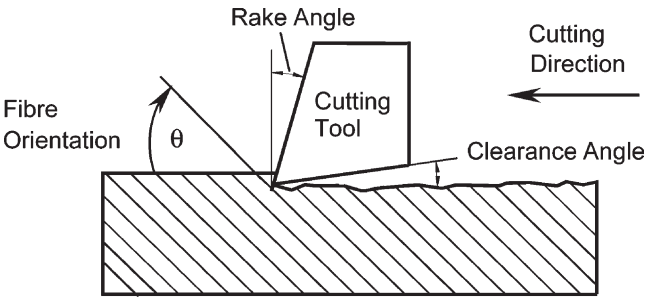

Fig. 1. The definitions of the cutting variable.

Table 1
Machining conditions for the F593 specimens

Fibre orientation (°)	0, 30, 60, 90, 120, 150
Rake angle (°)	–20, 0, 20, 40
Depth of cut (mm)	0.001, 0.050, 0.100

9257B, which was attached to the hydraulic table. The cutting speed was fixed at 1 m/min.

Two commercial resin systems, the F593 and MTM56 prepregs, were used in the experiment. To investigate the effect of cutting conditions on machinability, the F593 prepregs were used to make unidirectional 4 mm thick carbon/epoxy panels, cured under the pressure of 0.6 MPa at the temperature of 177°C for 2 h. These panels, with the dimensions of 300 mm×500 mm, were then cut into specimens of the dimensions of 15 mm×45 mm with the desired fibre orientation for the cutting experiment. The fibre orientation, θ, is defined clockwise with respect to the cutting direction, as shown in Fig. 1. The cutting tools used were made from tungsten carbide with a clearance angle of 7° and rake angles from −20° to 40°. Table 1 lists the cutting conditions. To examine the effect of the ratio of depths of cut to fibre diameter, the machinability at small depths of cut was also investigated.

In studying the influence of curing conditions, the MTM56 prepregs were used because the F593 prepregs were not available in the market at the stage of the experiment. Table 2 lists the cure procedures under the pressure of 0.62 MPa. The temperature in each cure procedure was increased at 3°C/min to the specified value, held at this value for the duration listed in Table 2 and then cooled down to room temperature. Procedure T2 is

Table 2
Curing conditions for making the MTM56 panels

Cure procedure	Temperature (°C)	Holding time (min)
T1 (under cure)	110	0
T2 (standard cure)	120	10
T3 (over cure)	120	20

Table 3
Machining conditions for the MTM56 specimens

Fibre orientation (°)	0, 30, 60, 90, 120, 150
Rake angle (°)	0
Depth of cut (mm)	0.025, 0.050, 0.075, 0.100, 0.125, 0.150, 0.175, 0.200, 0.250
Cure procedure	T1, T2, T3

a standard cure cycle recommended by the manufacturer of the MTM56 prepregs. Procedure T1 led to under-cured components and Procedure T3 gave rise to over-cured products. Table 3 lists the cutting conditions used for the MTM56 specimens.

The surface roughness of a machined surface was measured using a profilometer (Mitutoyo, Surftest 402 Series 178, cut-off=0.8 mm). The morphology of the machined surface was observed using an optical microscope (Leica LEITZ DMRXE) and a scanning electron microscope (SEM) Philips XL-30.

3. Results and discussion

3.1. Surface roughness

The surface roughness of the machined specimens made of F593 panels is presented in Fig. 2, which shows the significant effect of the fibre orientation of the composite, θ. It is clear that there exists a threshold, θ =

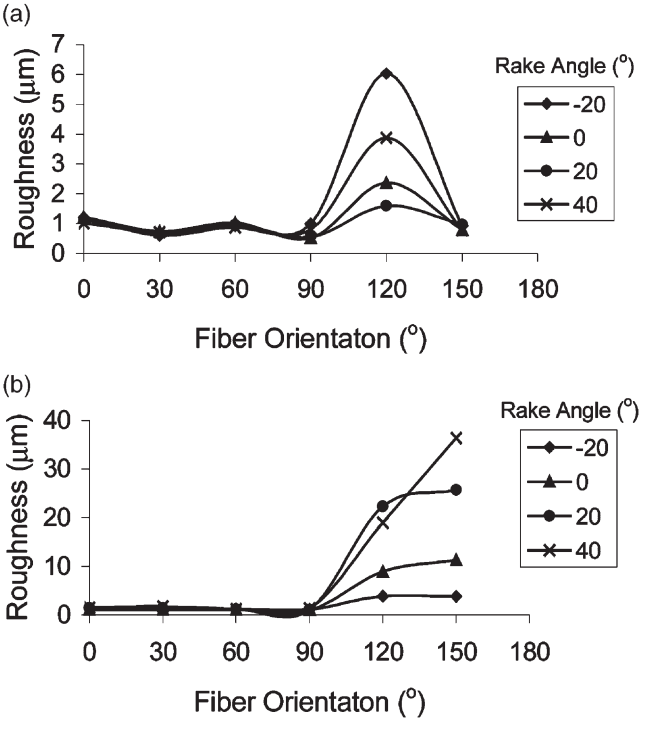

Fig. 2. Effect of fibre orientation on surface roughness (F593 panels). The depths of the cut were (a) 0.001 mm, (b) 0.050 mm.

90°, beyond which the surface roughness varies remarkably. Under a given depth of cut smaller than the fibre diameter (7 μm–9 μm), 1 μm for example, the surface roughness increases sharply when $\theta > 90°$ but decreases again when θ reaches 120°. Before reaching the threshold of 90°, the change of the surface roughness is small, ranging from 0.6 μm to 1.2 μm, and the effects of rake angle and fibre orientation are minor. At the most unfavourable fibre orientation of 120°, the surface roughness shows little dependence on the rake angle, γ_0, with the best surface finish at $\gamma_0 = 20°$ and the worst at $\gamma_0 = -20°$.

When the depth of cut becomes larger than the fibre diameter, a different mechanism seems to occur. For instance, at the depth of cut of 50 μm the surface roughness does not decrease when θ is over 120°, as shown in Fig. 2(b). The rake angle effect becomes greater and a sharper cutting tool (larger positive γ_0) produces a rougher surface. However, it is still true that $\theta = 90°$ is a critical angle, below which the effects of rake angle and fibre orientation are trivial. In this case, the surface roughness is in the range of 1 μm to 1.5 μm and is comparable to that when the depth of cut is smaller than the fibre diameter.

The above phenomenon may be explained by the variation of deformation mechanisms in the cutting zone when the depths of cut and fibre orientation change, as schematically illustrated in Fig. 3 using a model with a single fibre. When θ is less than 90°, as shown in Fig. 3(a), regardless of the depth of cut, the fibre is pushed by the tool (force F_1) in the direction perpendicular to the fibre axis and toward the workpiece subsurface. In this case, the fibre is better supported by the material behind and hence the bending of the fibre can be small. Meanwhile, the force component along the fibre axis (F_2) creates a tensile stress to make the fibre easier to break in the neighbourhood of the cutting zone. This is because carbon fibres are brittle and can fracture easily under tension. As a result, the surface roughness and subsurface damage are small, as shown in Fig. 2 and the micrographs (Figs. 11–14). When $\theta > 90°$, the situation becomes more complicated. When the depth of cut is less than $d \sin(\theta - 90°)$, where d is the fibre diameter, i.e., when the tool is cutting at the end surface of the fibre as illustrated in Fig. 3(b), the fibre is subjected to an axial compression. In this case, it is unlikely to break when the surrounding epoxy, which is quite brittle, is fractured. Thus a machined surface normally has many protruded fibres that results in a greater surface roughness. When the depth of cut becomes larger than $d \sin(\theta - 90^o)$, the tool exerts a different set of forces on the fibre, as shown in Fig. 3(c). The pushing force (F_1) perpendicular to the fibre axis is towards the external of the workpiece and hence the fibre gets a weaker support from the surrounding materials, leading to a more severe fibre bending and fibre-matrix debonding. This, in turn, causes a rougher surface finish and deeper subsurface damage. Hence, the mechanism of the surface roughness generation varies with the fibre orientation. This will be further discussed in Section 3.4.

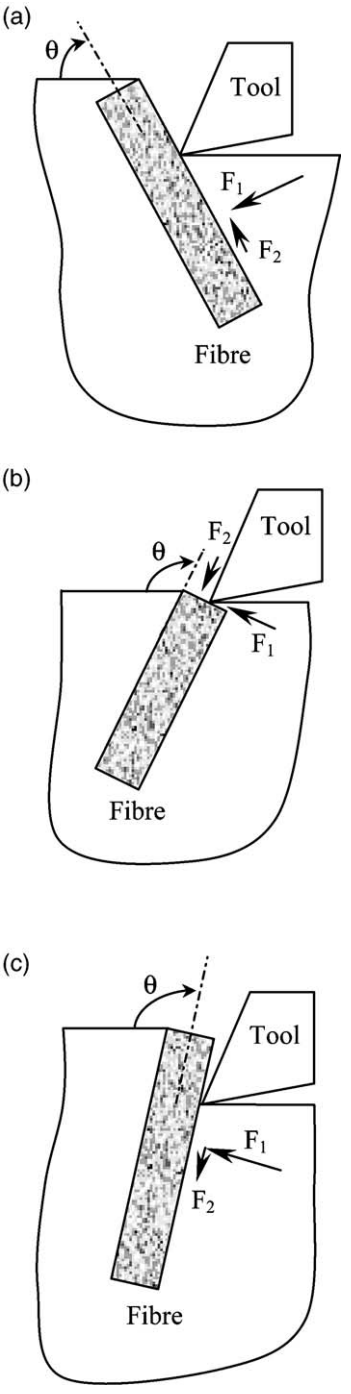

Fig. 3. Schematic cutting models.

3.2. Cutting forces

For convenience, the cutting forces along and perpendicular to the cutting direction are called the horizontal

and vertical forces, respectively. Figs. 4–7 demonstrate the variation of the forces with the rake angle, fibre orientation and depth of cut.

The rake angle effect is not so significant when compared with the influence of the other two variables. At a small depth of cut (e.g. 1 μm), a rake angle between 0° and 20° gives rise to small cutting forces (Fig. 4). At a larger depths of cut (e.g. 50 μm), the horizontal force decreases slightly as the rake angle increases except the cases with θ = 120° and 150° (Fig. 5). These are related to the resultant force variation when the fibre orientation and rake angle change. An interesting phenomenon is that the vertical forces at the fibre orientations of 120° and 150° decrease with the increment of rake angle (Fig. 5(b)). This is understandable when the mechanics model in Fig. 3(c) is recalled. At a greater fibre orientation, a larger rake angle and a higher depth of cut, the workpiece material applies a pulling force to the tool and hence the vertical cutting force becomes negative, as shown in Figs. 5(b) and 7(b). When this happens, the quality of the machined workpiece, including the surface roughness and subsurface damage, becomes poor, as show in Figs. 2, 13–15 to be discussed later.

The fibre orientation greatly influences the cutting forces as shown in Figs. 6–7. At a small depth of cut (e.g. 1 μm, Fig. 6), both the horizontal and vertical forces increase as θ increases, decrease when θ reaches 60°, and increase again after 120°. In the case with the depths of cut of 50 μm and 100 μm, the horizontal force continuously increases until θ = 120° (Fig. 7(a)).

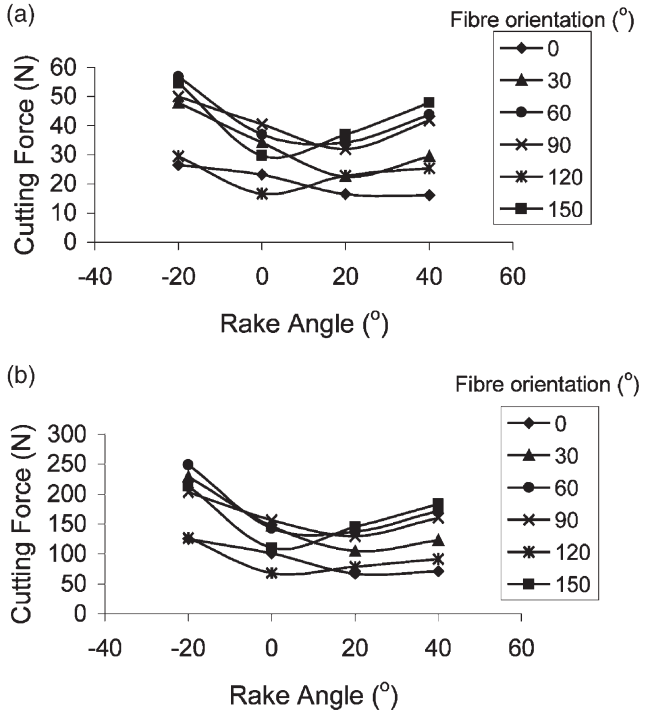

Fig. 4. Rake angle effect on (a) horizontal force, (b) vertical force (F593 panels, depth of cut=0.001 mm).

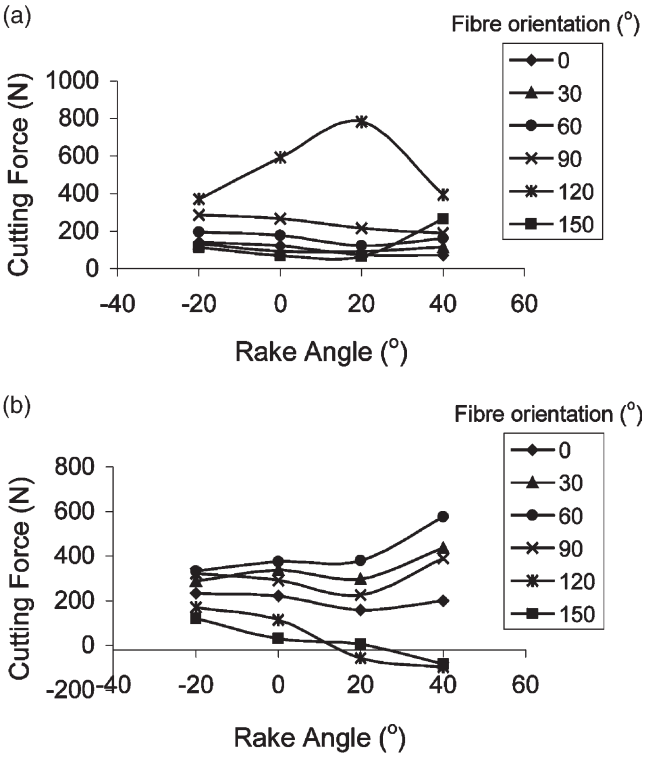

Fig. 5. Rake angle effect on (a) horizontal force, (b) vertical force (F593 panels, depth of cut=0.050 mm).

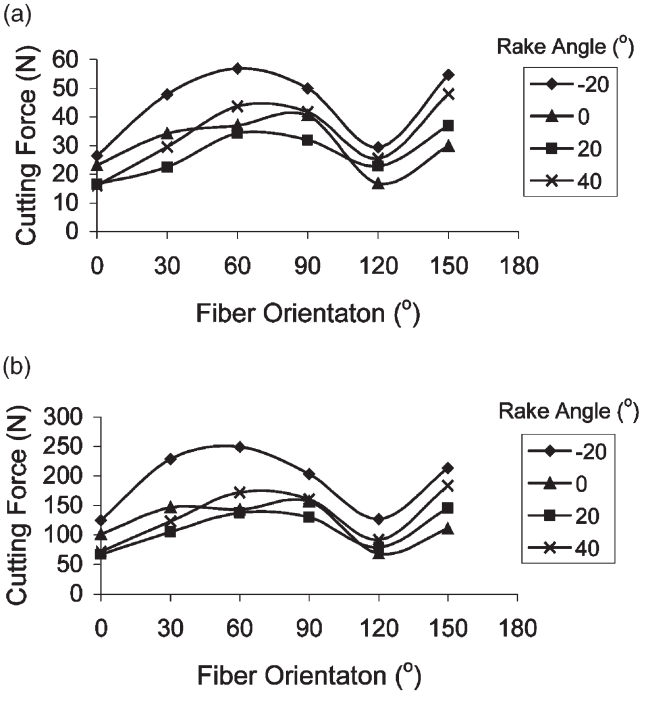

Fig. 6. Fibre orientation effect on (a) horizontal force, (b) vertical force (F593 panels, depth of cut=0.001 mm).

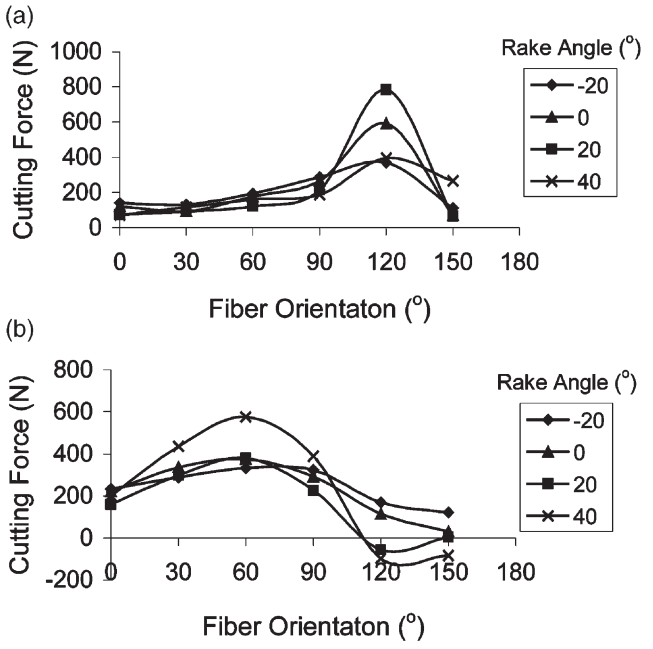

Fig. 7. Fibre orientation effect on (a) horizontal force, (b) vertical force (F593 panels, depth of cut=0.050 mm).

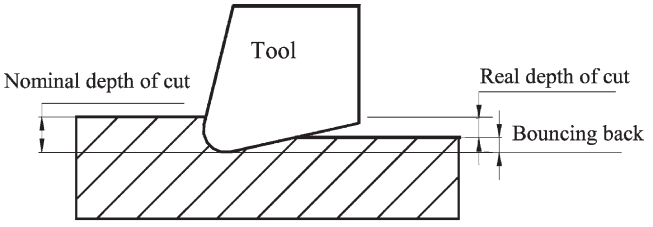

Fig. 8. An illustration of the bouncing back after cutting.

3.3. Bouncing back

It was found that the real depth of cut and nominal depth of cut are very different in cutting FRPs, as shown in Figs. 8 and 9. This happens when a part of the material in the cutting path was pushed down during the cutting but sprang back partially elastically after the tool passed away. Fig. 10 shows the cutting force variation with the nominal depth of cut. Because of the bouncing back, the vertical cutting force increases with a distinguished slope corresponding to the increase of the bouncing back thickness (Fig. 9). When the nominal depth of cut reaches a certain value, 100 μm in the current case, the magnitude of the bouncing back does not change much further and as a result the increasing rate of the normal cutting force also become very small. Fig. 10 also shows that the dependence of the horizontal cutting force on the bouncing back is not strong, although the effect is still clear. All these indicate that the bouncing back is a key factor that contributes to the generation of the cutting forces.

It was found that the magnitude of bouncing back is related to the radius of a cutting tool, when all the other cutting conditions are the same. A series of measurements showed that when the fibre orientation $\theta < 90°$, the magnitude of bouncing back is equal to or slightly greater than the tool radius. If $\theta > 90°$, the magnitude of the bouncing back can be up to more than twice the tool radius, depending on the θ value. As discussed in the previous section and illustrated in Fig. 3, this is because at a greater θ value, many fibres were pushed to bend (but not break at the cutting point). When the cutting tool passed away, these fibres recovered elastically so that the magnitude of the bouncing back becomes large.

3.4. Subsurface damage

Under some specific cutting conditions, the subsurface of a machined specimen can be damage-free, as shown in Fig. 11, but under some other conditions, debonding and fibre-breakage can take place easily, as shown in Figs. 12 and 13. The subsurface damage is related to the depth of cut, fibre orientation and rake angle. The observation shows that in general a smaller depth of cut generates less subsurface damage. At a larger depth of cut (e.g. 50 μm and 100 μm), the subsurface damage becomes more severe when the fibre orientation is

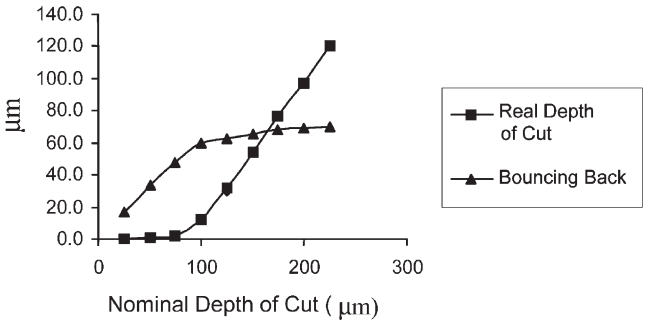

Fig. 9. Relationship among the nominal depth of cut, bouncing back and real depth of cut (MTM56 panels, fibre orientation=30°).

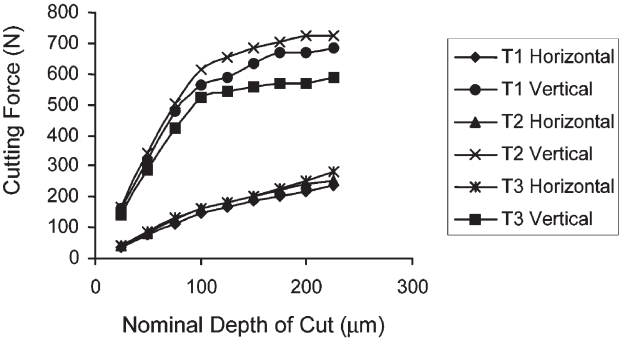

Fig. 10. Effect of the depth of cut and curing conditions on the cutting forces (MTM56 panels, fibre orientation=30°).

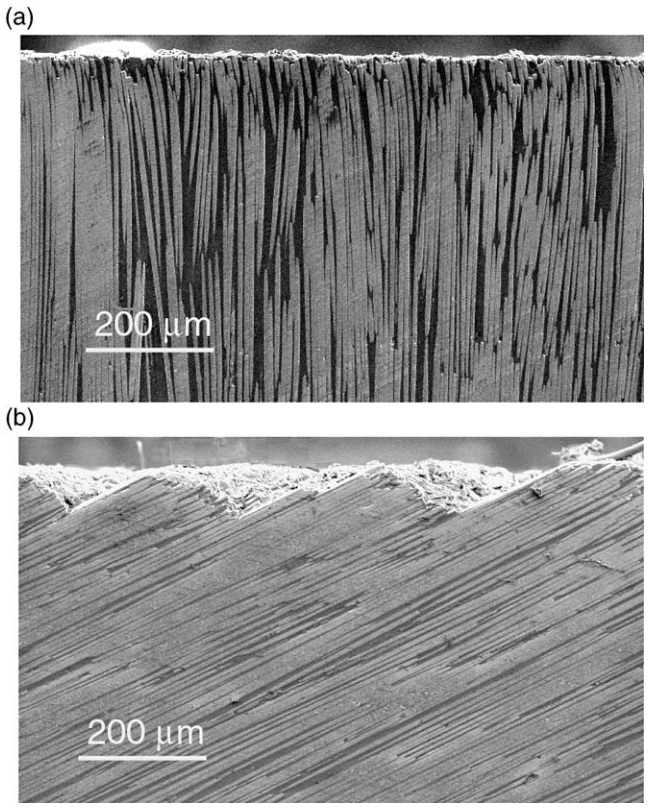

Fig. 11. Microstructure in the subsurface of F593 specimens (a) rake angle=20°, depth of cut=0.100 mm and fibre orientation=90°, (b) rake angle=20, depth of cut=0.050 mm and fibre orientation=150°.

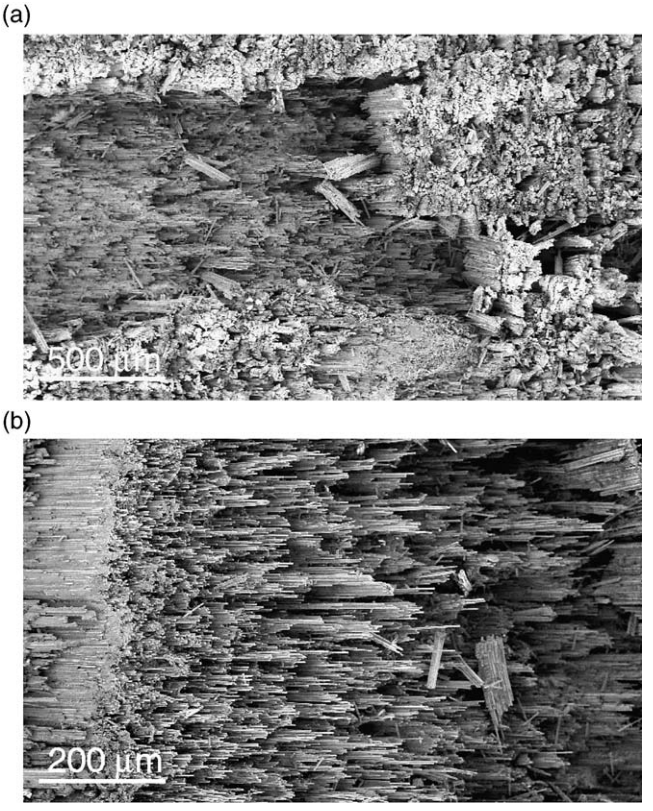

Fig. 13. Cracks and damages on machined specimens (F593 panels, fibre orientation=150°, rake angle=40°), (a) depths of cut=0.050 mm, (b) depths of cut=0.100 mm.

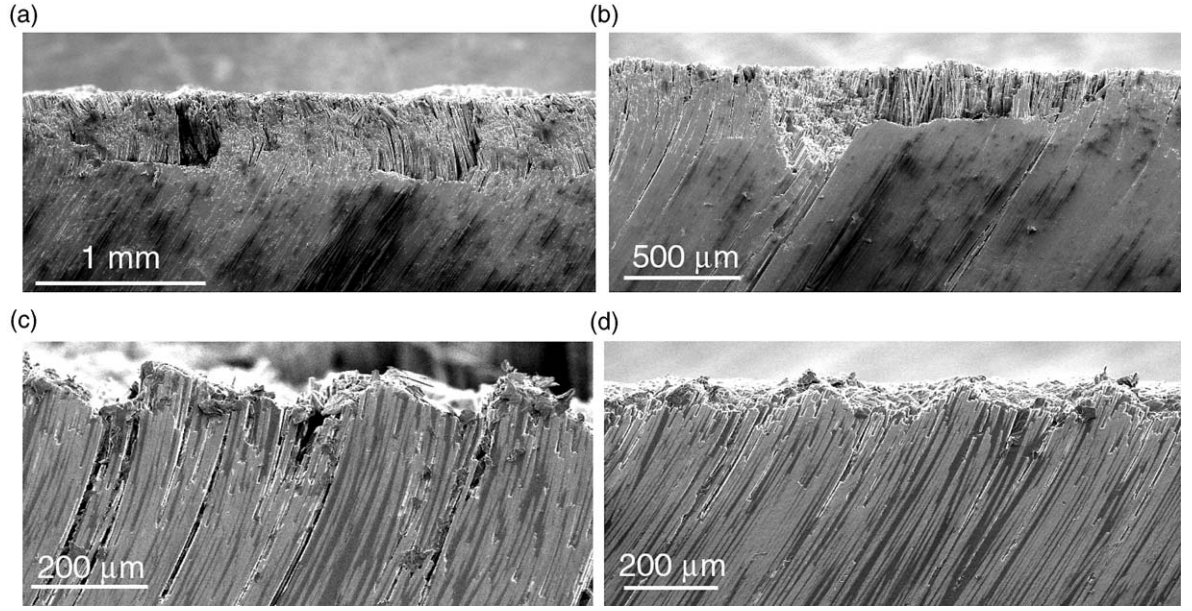

Fig. 12. Microstructure in the subsurface of F593 specimens (fibre orientation=120° and depth of cut=0.100 mm), (a) rake angle=–20°, (b) rake angle=0°, (c) rake angle=20°, (d) rake angle=40°.

between 120° and 150°. This explains why the surface roughness under these cutting conditions is also high. The fibre orientation plays a key role here. For instance, when $\theta = 150°$, subsurface cracks appear only at the rake angle of 40°; but when $\theta = 120°$, cracking always occurs regardless of the rake angle value. It is interesting to note that under different depths of cut, e.g. 50 μm and 100 μm, the subsurface has a similar feature if the fibre orientation and rake angle are the same. This seems to indicate that the depth of cut does not play a critical role here.

The SEM examination of the machined surfaces leads to the conclusions that are in agreement with the surface roughness observations. When $\theta \leq 90°$, a machined surface is not influenced much by the fibre orientation, depth of cut and rake angle. Fig. 14(a) shows a typical surface machined at the fibre orientation of 0°, depth of cut of 100 μm and rake angle of 20°. Some fibres were damaged during machining, fuzzing appeared, but the damage was localised in the very vicinity of the surface. Fig. 14(b) presents another type of machined surface with $\theta = 90°$, depth of cut of 100 μm and rake angle of 20°. Although the surfaces in Fig. 14(a) and (b) have the same roughness of 1 μm, they have different surface integrity due to their difference in fibre orientation. When $\theta > 90°$, the machined surface integrity becomes dependent on all the variables, i.e. rake angle, depth of cut and fibre orientation.

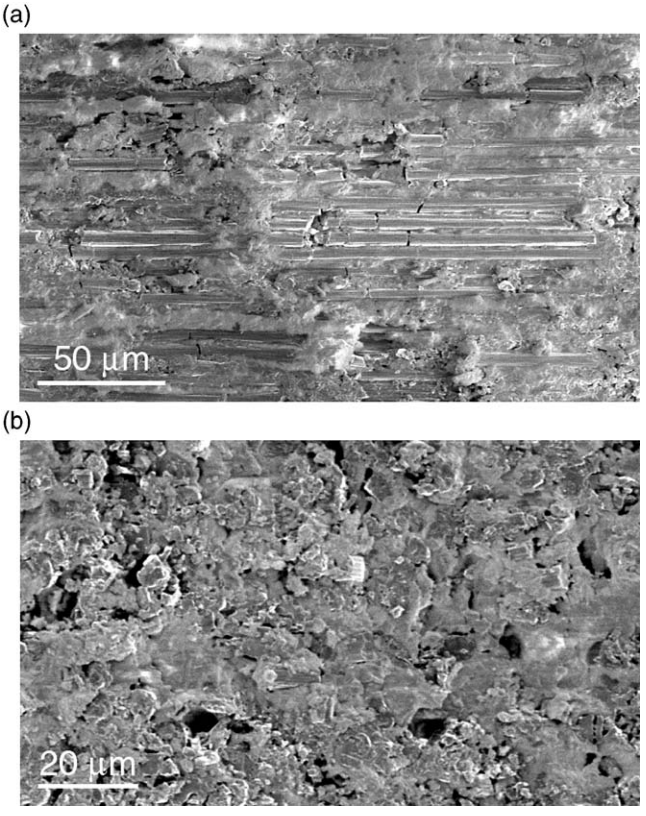

Fig. 14. Dependence of surface quality on the fibre-orientation (F593 panels, depth of cut=0.100 mm, rake angle=20°) (a) fibre orientation=0°, (b) fibre orientation=90°.

3.5. Effect of curing conditions

The mechanical properties of the F593 panels were provided by the manufacturer, as listed in Table 4. The tensile tests on MTM56 panels were conducted in the authors' laboratory and the results are listed in Table 5. Clearly, the mechanical properties of the MTM56 panels are affected by the curing conditions. The best tensile strength was obtained by the standard curing procedure. The under cure leads to 90% of the tensile strength from the standard cure in the fibre direction and 75% in the transverse direction. The over cured specimen has only 76% of the tensile strength in the fibre direction and 60% in the transverse direction. On the other hand, however, the best elastic modulus was obtained by the under cure, which, compared to that from the standard one, is 105% in the fibre direction and 111% in the transverse direction. The over cure procedure gives 91% and 98%, respectively. Curing conditions do not show noticeable effect on the surface roughness after machining (Fig. 15).

The effects of the cure degree on the cutting forces are shown in Fig. 10. It can be seen that the horizontal cutting force is generally unaffected by cure conditions. The variation of the vertical cutting force with the cure conditions is similar to that of the tensile strengths of the materials.

The cure degree alters the microstructure of the MTM56 panels (Fig. 16). Compared with the standard cure, both the under cure and over cure introduce subsurface defects during the manufacturing of the composites. As shown in Fig. 16, the matrix may disappear in some areas (typically 50×200 μm). However no other significant differences were found. This shows the reason that the cutting forces are weak functions of the curing conditions.

4. Conclusions

This investigation achieves an understanding of the mechanisms of machinability of unidirectional FRPs and leads to the following conclusions:

1. Fibre orientation, θ, is a key factor that determines

Table 4
Mechanical properties of the F593 specimens

Tensile strength (MPa)	1331
Tensile modulus (GPa)	120.0
Compression strength (MPa)	1655
Compression modulus (GPa)	114.5

Table 5
Mechanical property variation of the MTM56 panels with curing conditions

Cure procedure	Type	Tensile strength (MPa)		Tensile modulus (GPa)	
		(MPa)	%	(MPa)	%
T1	Longitudinal	1623	90	275.9	105
T1	Transverse	21.3	75	25.7	111
T2	Longitudinal	1806	100	261.6	100
T2	Transverse	28.5	100	23.2	100
T3	Longitudinal	1385	76	236.9	91
T3	Transverse	17.0	60	22.8	98

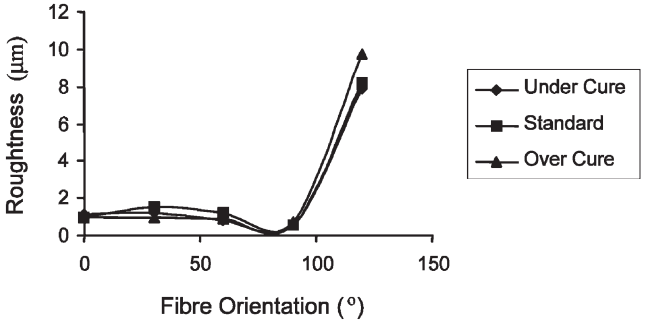

Fig. 15. Effect of curing conditions on the surface roughness (MTM56 panels, depth of cut=0.050 mm).

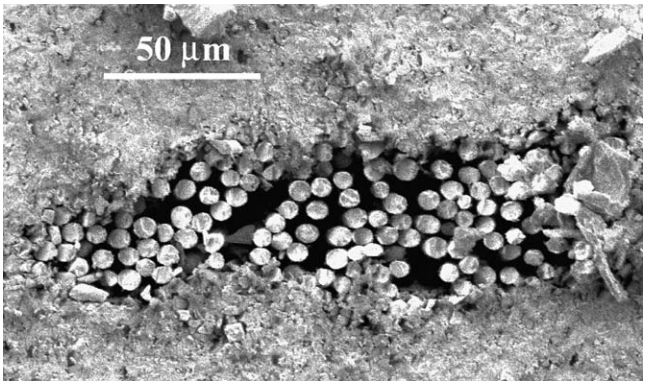

Fig. 16. Defects in an MTM56 specimen due to inappropriate curing conditions.

the surface integrity of a machined component. θ = 90° is a critical angle, beyond which a severe subsurface damage will occur.

2. The significant bouncing back of materials after cutting is a characteristic phenomenon associated with the machining of FRPs. The mechanism is the elastic bending of the high strength fibres.
3. When $\theta \leq 90°$, three distinct deformation zones appear, i.e., chipping, pressing and bouncing. However, if $\theta > 90°$, fibre-bending during cutting will become more significant. In this case, the cutting mechanism becomes more complicated.
4. The rake angle of a cutting tool, γ_0, affects only slightly the surface roughness. In the range studied, a better surface will be obtained when $0° < \gamma_0 < 20°$.
5. The cure conditions for making the FRPs alter their mechanical properties, particularly in the transverse direction. While the cure degree does not influence the surface roughness, it contributes slightly to the change of the cutting forces.

Acknowledgements

This work was supported by an ARC Large Grant.

References

[1] K. Colligan, M. Ramulu, The effect of edge trimming on composite surface plies, Manufact. Rev. 5 (4) (1992) 274–283.
[2] D.H. Wang, M. Ramulu, D. Arola, Orthogonal cutting mechanisms of graphite/epoxy composite. Part I: Unidirectional laminate. Int, J. Mach. Tools Manufact. 35 (12) (1995) 1632–1638.
[3] S.O. An, E.S. Lee, S.L. Noh, A study on the cutting characteristics of glass fibre reinforced plastics with respect to tool materials and geometries, J. Mater. Processing Technol. 68 (1997) 60–70.
[4] J.H. Lee, D.E. Kim, S.J. Lee, Statistical analysis of cutting force ratios for flank-wear monitoring, J. Mater. Processing Technol. 74 (1998) 104–114.
[5] M. Ramulu, Machining and surface integrity of fibre-reinforced plastic composites, Sadhana 22 (3) (1997) 449–472.
[6] N. Bhatnagar, N. Ramakrishana, N.K. Nail, R. Komanduri, On the machining of fibre reinforced plastic (FRP) composite laminates. Int, J. Mach. Tools Manufact. 35 (5) (1985) 701–716.
[7] H.Y. Pwu, H. Hocheng, Chip formation model of cutting fibre-reinforced plastics perpendicular to fibre axis, Trans. ASME 120 (1998) 192–196.
[8] H. Zhang, W. Chen, D. Chen, L. Zhang, Assessment of the exit defects in carbon fibre-reinforced plastic plates caused by drilling, Key Engng Mater. 196 (2001) 43–52.
[9] G. Caprino, L. Santo, L. Nele, Interpretation of size effect in orthogonal machining of composite materials. Part I: Unidirectional glass-fibre-reinforced plastics, Composites Part A 29A (1998) 887–892.